

Meteorological forecasting for the European Southern Observatory in Chile

R. DEIDDA⁽¹⁾, M. MARROCU⁽¹⁾ and A. SPERANZA⁽²⁾

⁽¹⁾ *CRS4, Centro di Ricerca, Sviluppo e Studi Superiori in Sardegna
C.P. 94, I-09010 Uta (Cagliari), Italy*

⁽²⁾ *Università di Camerino, Dipartimento di Matematica e Fisica
Via Madonna delle Carceri, I-62032 Camerino, Italy*

(ricevuto il 19 Giugno 1998; revisionato il 7 Ottobre 1999; approvato il 27 Ottobre 1999)

Summary. — The potential of numerical weather prediction to supply a useful support to flexible scheduling of astronomical observations is investigated. We applied some common tools presently used in numerical meteorology at regional scale in order to evaluate the ability to forecast local meteorological conditions (cloud cover, air temperature and wind speed) at Cerro Paranal and Cerro La Silla in Chile, where telescopes of ESO (the European Southern Observatory) are sited. The first part of this paper is devoted to evaluating the accuracy of analysis and forecasts of the ECMWF (European Center for Medium-range Weather Forecast) general circulation model for ESO needs. With this aim, analysis and 24-48 hour forecasts from ECMWF are systematically compared with observations at the ground meteorological stations of Paranal and La Silla, and with vertical profiles of radiosounding launches at Antofagasta and Quintero. The second part of this paper is aimed at improving the ECMWF forecasts at telescope sites by means of Kalman filter statistical post-processing and meteorological limited area modeling. Encouraging results are obtained concerning temperature, whereas much less satisfactory results are obtained for wind field and cloud cover. The most critical aspects of atmospheric dynamics affecting the local forecast are discussed within the limits of available information.

PACS 92.60 – Meteorology.

PACS 95.85 – Astronomical observations.

1. – Introduction

Reliable weather forecasts can significantly contribute to the optimization and to a more efficient scheduling of astronomical observations. Forecasts of cloudiness and water vapor content can provide a useful support in scheduling photometric or infrared night observations; the forecast of temperature at ground level can be used to preset air temperature within the dome so that the mirror telescope is in thermal equilibrium with the external temperature at the dome opening; the forecast of extreme wind speed at the height of the telescope is of great utility in reducing the problem of interrupting

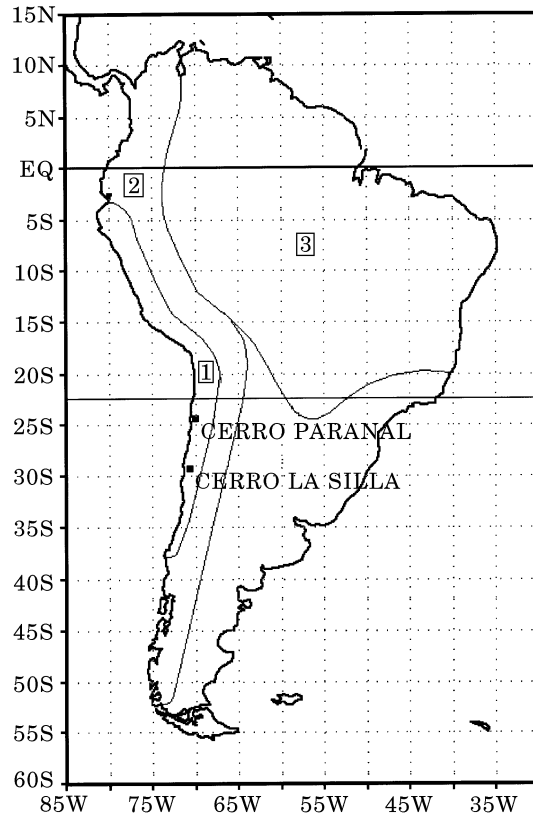


Fig. 1. – The three different climate areas in the southern tropical belt of South America. Region 1 is characterized by an arid climate, region 2 by a mountain climate and region 3 by a tropical climate. The position of the two ESO sites (Cerro Paranal and Cerro La Silla) is also shown.

observations in course, thereby reducing loss of time and money and preserving the structure of the telescope. Another parameter that is useful to know in advance is the atmospheric seeing which is related to the distribution of turbulence along the observation path [1].

The meteorological part of these topics has been the subject of a feasibility study partially financed by the European Southern Observatory (ESO) [2-4], the main scientific results of which we describe in this paper. More specifically, our research addressed to “short range” (12 to 72 hours in advance) forecasting of atmospheric conditions (in particular cloud cover, wind speed and temperature) at Cerro La Silla and Cerro Paranal in Chile (see fig. 1).

The two sites are located at sub-tropical latitude along the western slope of the Andes, in a narrow strip characterized by an arid climate. This strip, together with another North-South elongated area of high mountain climate, separates the Pacific Ocean from the pluvial-tropical region extending over the entire northern portion of South America (again, see fig. 1). Water vapor, vertically mixed by tropical convective activity, tends to be trapped by strong inversions over the coastal ocean and extratropical (middle-latitude) perturbations seldom penetrate so far north. As a

consequence, the local climate is essentially arid. On occasion, however, particularly deep extratropical troughs can bring the middle-latitude jet stream of the southern hemisphere to the latitude of the two considered sites and, given their altitude, cause adverse atmospheric conditions. It is clear that any short-range forecasting procedure for the site in question must start from an adequate forecast of the "weather perturbations" which are the primary generators of changes in the atmospheric conditions of interest for astronomical activity, but must take into account, as well, local agents (topography, heat sources, etc.) which also play an important role in the local forcing of atmospheric conditions. This can be done in different ways, and the analysis of some alternative forecasting approaches specifically finalized to ESO activities was the object of the feasibility study.

Modern short-range weather forecasting is developed through a procedural chain which, almost invariably, starts from a planetary-scale numerical forecast obtained by a general circulation model (GCM) in which the laws of atmospheric motion (from solar heating, to air motion, to viscous dissipation) are explicitly represented on a numerical grid: processes determining atmospheric evolution on a time-scale of the order of one day develop, in fact, on the planetary scale. Such models have been set up and are currently used with the specific purpose of forecasting the global evolution of the atmosphere and, as such, are optimized with respect to the global variance of meteorological fields (pressure, temperature, winds, etc.). As a consequence, a GCM forecast is usually not suited for local forecasting even where space-time numerical resolution seems adequate.

In order to perform local forecasts, starting from predictions of a GCM, it is usually necessary to insert additional steps in the procedural chain. A preliminary step consists in comparing the global analysis of meteorological fields, released by the same centers issuing the global forecast, with local meteorological information as provided by the local observational network. Surprising as it may seem, we do not expect the analysis to coincide with observations at specific stations, even if the observations themselves have been used in the analysis (which is not the case here). The reason is the same mentioned above: also the analysis, as the global forecast, results from an optimization process aimed at representing the global fields and not local details. The gap between global analysis/forecast and local meteorological conditions can be filled with phenomenological-statistical techniques as well as with more locally adapted numerical models (typically the so-called limited area models, LAMs).

In this paper we describe our analysis of the meteorological conditions at ESO sites in terms of the above-described procedure. In sect. **2** the data sets analyzed and used in this study are presented. In sect. **3** we discuss the comparison of direct observations at the ESO sites with the ECMWF analysis. In sect. **4** we analyze ECMWF short-range forecasts and compare them with local meteorological observations. In sect. **5** we propose possible improvements of the ECMWF forecasts using statistical post-processing based on Kalman filtering. In sect. **6** we discuss the results of some numerical integrations of a limited area model nested into the GCM of ECMWF. In sect. **7** we draw our conclusions.

2. – Data sets

In this study we used daily ECMWF meteorological analysis at synoptic hours (00, 06, 12 and 18 GMT) and 24-48 hours forecasts (starting at 12 GMT) from 1989 to 1993 in

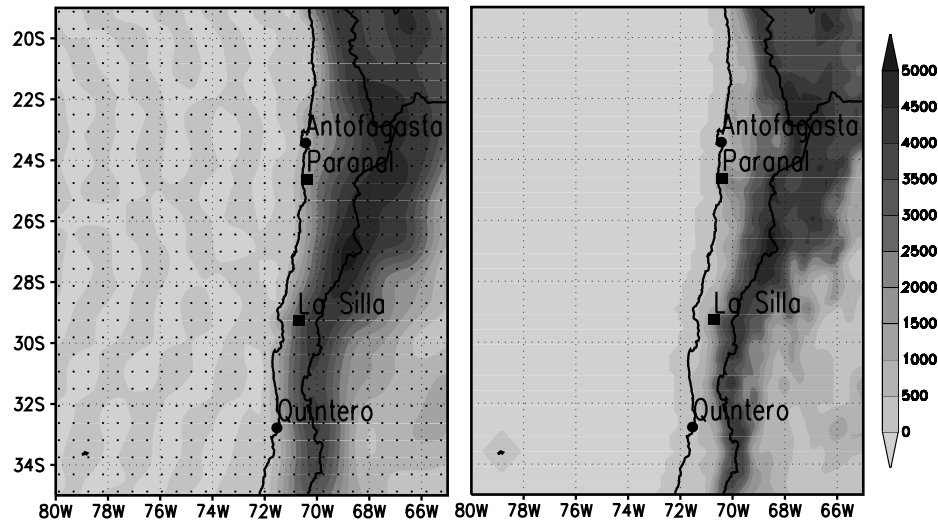


Fig. 2. – Left: ECMWF orography (meters) at the horizontal resolution of 0.5625 degree and the corresponding grid-point mask; right: orography (meters) used for LAM simulations derived from NCAR orography at one sixth degree of resolution. In both maps locations of Antofagasta, Paranal, La Silla, and Quintero are also shown.

an area covering the entire Chile. The horizontal resolution of the grid is 1.125 degrees (about 120 km at Chilean latitudes) during the period from 01/01/89 to 16/09/91 and 0.5625 degrees (about 60 km) from 17/09/91 to 31/12/93. In fig. 2 (left) we show the whole ECMWF grid at the 0.5625 degree resolution together with the orography in the domain of interest, while in fig. 3 (left) a cross-section at Paranal latitude is shown.

The ECMWF data set was composed of upper air fields available over 15 pressure levels together with several surface fields. Upper air fields are: geopotential height, temperature, relative humidity and components of wind velocity. Surface fields are:

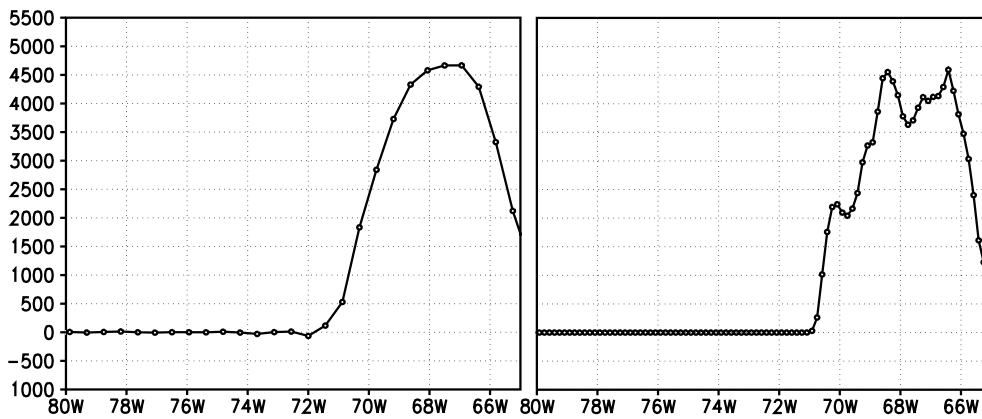


Fig. 3. – Comparisons between W-E orography sections (meters) at Paranal latitude; left: section of the orography of the ECMWF model; right: section of the orography used for LAM simulations.

TABLE I. – *Geographical information about La Silla and Paranal, where surface meteorological stations are located, about Antofagasta and Quintero, where balloons for radiosounding are released, and about nearest points (NP) in the ECMWF grid.*

	Meteo stations		Radiosoundings	
	La Silla	Paranal	Antofagasta	Quintero
Altitude	2400 m	2636 m		
Longitude	70W42	70W24	70W26	71W32
latitude	29S16	24S37	23S26	32S47
Distance from coast	40 km	12 km		
NP altitude	2680 m	1835 m	1294 m	1182 m
NP longitude	70W52.5	70W18.75	70W18.75	71W26.25
NP Latitude	29S15	24S45	23S37.5	32S37.5
Distance from NP	17 km	17 km	25 km	20 km

total cloud cover, supplementary total cloud cover, 2-meter temperature, 10-meter wind, surface pressure, orography and some other fields needed for LAM initialization and boundary conditions.

Local observations and measurements at the astronomical sites in Chile, consisting of meteorological observations in La Silla and Paranal and vertical profiles from radiosoundings in Antofagasta and Quintero, were also available through ESO in order to perform comparisons with ECMWF analysis and forecasts. More specifically, the local data set collects: i) observations of cloud cover in Paranal at 0, 2, 4, 6, 8, 10 GMT from 2/6/92 to 31/12/93; ii) surface meteorological parameters (10-meter wind speed and direction, 2-meter air temperature) in Paranal and La Silla, every 20 minutes from 1/10/89 to 30/09/94; iii) vertical profiles of temperature and wind speed from radiosonde launches in Antofagasta and Quintero at 12 GMT from 1/1/85 to 30/06/94. Before collecting all these data into a single and easy-to-access database, we performed some checks of internal consistency and eliminated some macroscopic errors. The observation sites are shown in fig. 2, in their geographical context; some information on the sites and on their nearest ECMWF grid points can be found in table I.

3. – Comparison of ECMWF analysis with local observations

In order to evaluate the limits of the analysis in representing local meteorological variability, we performed a systematic comparison between ECMWF analysis and meteorological observations. In particular, we compared: vertical profiles at Antofagasta and Quintero with profiles extracted from ECMWF analysis; visibility observations in Paranal with ECMWF supplementary total cloud cover fields and with estimates based on ECMWF relative humidity fields; 2-meter temperature and 10-meter wind speed observed at meteorological stations in La Silla and Paranal with the corresponding variables in ECMWF analysis. The period selected for all comparisons is the entire year 1993. The ECMWF grid resolution for this period is 0.5625 degrees, as shown in fig. 2 (left).

TABLE II. – Average of daily correlations (r), mean errors ($\bar{\epsilon}$), and mean absolute errors ($|\bar{\epsilon}|$) between vertical profiles from radiosoundings in 1993 and the corresponding profiles obtained by bilinear interpolation of grid values from ECMWF analysis and 24-48 hour forecast. The averages of absolute errors on temperature profiles are also shown for the whole 89–93 period.

Radiosoundings	ECMWF profile	1993			89–93
		r	$\bar{\epsilon}$	$ \bar{\epsilon} $	$ \bar{\epsilon} $
Antofagasta 12 GMT Temperature (°C)	Analysis	0.986	1.39	2.54	2.50
	24 h forecast	0.985	1.41	3.00	2.91
	48 h forecast	0.984	1.32	3.24	3.11
Quintero 12 GMT Temperature (°C)	Analysis	0.991	1.15	2.48	2.52
	24 h forecast	0.989	1.35	3.39	3.25
	48 h forecast	0.988	1.37	3.96	3.71
Antofagasta 12 GMT Wind (m/s)	Analysis	0.918	–0.36	2.11	
	24 h forecast	0.813	–3.36	4.31	
	48 h forecast	0.781	–0.24	5.09	
Quintero 12 GMT Wind (m/s)	Analysis	0.854	1.04	4.26	
	24 h forecast	0.785	0.95	6.13	
	48 h forecast	0.748	1.05	7.24	

3.1. Vertical profile comparisons. – Radiosoundings of temperature and wind velocity derived from balloon launches at Antofagasta and Quintero (daily at 12 GMT) were compared with the corresponding vertical profiles extracted from ECMWF analysis. These last profiles have been obtained by bilinear interpolations (on each pressure level where ECMWF data are available) of the four values at the nearest grid points to Antofagasta or Quintero, and then by a vertical cubic spline to extract the comparing values at the same pressure levels at which the balloons recorded the measurements. Results of these comparisons are summarized in table II in terms of correlations, mean errors and mean absolute errors between the vertically interpolated analysis values and the vertical profiles from radiosoundings for each launch in 1993.

The comparisons of wind speed profiles in Quintero revealed some anomalies in the ECMWF data set. Figures 4 show plots of correlations, mean errors and mean absolute errors of winds in 1993. A different behaviour before and after March 1993 is evident. After some investigation it was discovered that the Quintero balloon soundings had not been used for wind analysis from March 1993 to March 1995 due to unacceptably large differences from the first guess. These differences suddenly came back into an acceptable range in April 1995, so the assumption is that some consistent errors in the measurement instruments were corrected.

3.2. Cloud cover comparisons. – Total cloud cover is one of the most difficult meteorological fields to forecast and analyze. Estimates of cloud cover in Paranal were performed for each day in 1993 at 0 and 6 GMT starting from supplementary total cloud cover fields and upper-air relative humidity fields of ECMWF analysis. Although total cloud cover was also available through ECMWF analysis, this field was not used here

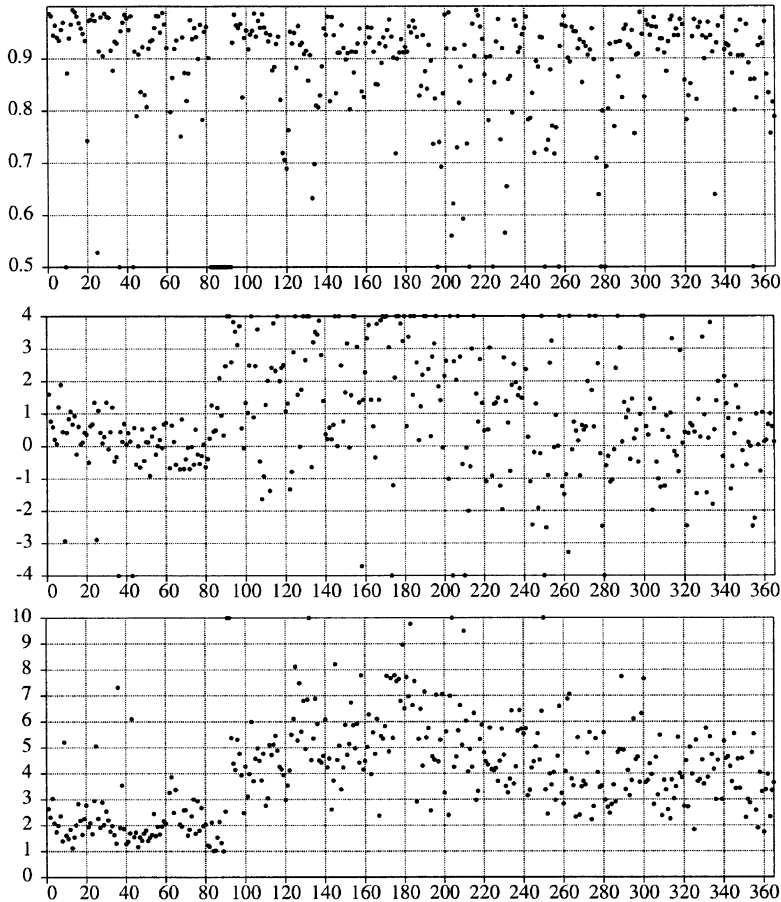


Fig. 4. – Daily (at 12 GMT) correlations (top), mean errors (middle), and mean absolute errors (bottom) between vertical profiles of wind velocity (m/s) from radiosoundings at Quintero in 1993 and the corresponding ECMWF analysis profiles interpolated at the site position.

since it is considered quite unreliable and classified as incorrect in ECMWF data documentation. One used instead the supplementary total cloud cover since it is a 6-hour forecast re-analyzed field. The upper-air relative humidity fields were considered since they are strictly related to cloud cover and can be used to construct an index of cloudiness.

Since the observed cloudiness cannot be considered as a local field related to only one grid-point variable, we have considered different ways to extract information from the ECMWF data. The best results were obtained by averaging the 25-point neighboring values of ECMWF, which correspond approximatively to a square area of side 250 km, centered in Paranal.

Several criteria were applied to estimate cloud cover in Paranal from ECMWF fields and the results of the comparisons with observed cloudiness are summarized in table III in terms of percentages of successful predictions of clear and cloudy sky. The skills of the cloudiness prediction based on indices computed from ECMWF fields are

TABLE III. – Percentages of success for cloud cover estimations at 0 and 6 GMT for different estimation criteria. E1 consists in guessing that the sky is always clear, E2 is the skill of the supplementary total cloud cover of the ECMWF analysis, and E3 is obtained using humidity upper-air field.

	E1	E2	E3
0 GMT	80%	82%	81%
6 GMT	81%	83%	85%

compared with those obtained by assuming that the sky in Paranal is always clear (criterion E1). This reasonable assumption is suggested by the altitude of the site and the local climatology, since Paranal is located in an arid region and most days of the year are clear: for example, in 1993 80–81% of the days were clear. Criterion E2 is based on ECMWF supplementary total cloud cover (2D field with values ranging from 0 to 1): we assume clear sky if the average resulting from the values of the 25 neighboring points is lower than 0.9, otherwise the sky is assumed cloudy. For the last criterion E3, the ECMWF relative humidity (3D upper-air field) is used: a mean vertical profile is computed by averaging the values of the 25 neighboring points in each pressure level; then the sky is assumed cloudy if in the mean vertical profile there are at least 3 levels (above the 500 mb) with more than 70% relative humidity, otherwise the sky is considered clear.

By using the ECMWF fields for estimating a cloudiness index with procedures E2 and E3 we are able to improve the percentage of success only marginally, with respect to the simple assumption that the sky in Paranal is always clear.

3.3. Two-meter temperature comparisons. – Errors between ECMWF analysis and observations of 2-meter temperature were systematically computed for the 1993 period. Considering the long autocorrelation time of the temperature field (typically on the order of two weeks), we first determined the error of the “24 h persistence model”, which consists in assuming that the 24-hour forecast of 2-meter temperature coincides with the value of the same variable observed 24 hours before. The skill of the persistence model in Paranal and La Silla stations is presented in table IV, columns A, in terms of correlations and averages of errors and of absolute errors at 00, 06, 12 and 18 GMT.

Next, we compared observations of 2-meter temperature with the corresponding values derived from ECMWF analysis by the bilinear interpolation of the 2-meter temperature field in the four grid points nearest to the station sites. It can be seen from columns B of table IV, by comparing mean ($\bar{\varepsilon}$) and absolute ($|\bar{\varepsilon}|$) deviation, that a great part of the error is a systematic error. This is an expected result, since analyzed data are referred to the altitude of the model which is quite different from the real altitude.

One way to correct such systematic error is to estimate 2-meter temperature by interpolating, at the altitude of the station, the vertical profiles of upper-air temperature resulting from the analysis. Although this simple approach has still the limitation that soil effects are not properly taken into account, results shown in columns C of table IV are considerably better than the previous ones: correlation

TABLE IV. – Correlations (r), mean errors ($\bar{\varepsilon}$), and mean absolute errors ($|\bar{\varepsilon}|$) between 2-meter temperature observations at La Silla and Paranal in 1993 and different estimates from ECMWF analysis at synoptic hours (H). Columns A: results of the “24 h persistence model”. Columns B: results using the 2-meter temperature field of ECMWF analysis; estimates are derived from bilinear interpolation of the 4 neighboring points in ECMWF grid. Columns C: results using the upper-air temperature profiles of ECMWF analysis; values are interpolated horizontally (at station position) and vertically (at station altitude).

Station	H	A		B			C		
		$ \bar{\varepsilon} $	r	$\bar{\varepsilon}$	$ \bar{\varepsilon} $	r	$\bar{\varepsilon}$	$ \bar{\varepsilon} $	r
Paranal	0	1.4	0.76	-1.2	1.8	0.67	0.8	1.3	0.81
	6	1.5	0.77	2.5	3.1	0.49	0.8	1.3	0.86
	12	1.6	0.77	2.1	2.8	0.53	0.2	1.0	0.90
	18	1.4	0.71	-5.8	5.8	0.73	-0.9	1.4	0.80
La Silla	0	1.9	0.79	4.3	4.3	0.85	-0.3	1.1	0.93
	6	1.9	0.80	8.8	8.9	0.58	-0.2	1.1	0.94
	12	1.7	0.79	8.1	8.1	0.59	-1.5	1.8	0.93
	18	1.8	0.81	-0.3	1.6	0.85	-1.4	1.7	0.93

exceeds 0.9 for La Silla and the mean absolute error is about 1.1 at 00 and 06 GMT. However, in all cases a sensible systematic error ($\bar{\varepsilon} \neq 0$) is still present.

3.4. Ten-meter wind velocity comparisons. – We performed the same kind of analysis described above on observations of 10-meter wind speed in Paranal and La Silla. We compared, in this case, measured 10-meter wind speed data with the bilinear interpolation at the station sites of the 10-meter wind speed field of ECMWF analysis. The agreement is, in this case, not very good: the mean absolute error is about 3 m/s, to be compared with a mean value of the field of about 6 m/s; correlations are 0.7, at most. Such a poor agreement is due to the fact that for this field the effects of soil and orography cannot be neglected. One way to account for these effects could be to re-analyze wind fields obtained from a forecast model at global scale with a “mass consistent model”, which is a diagnostic model specifically designed for representing the effects of orography on wind field flows averaged over time intervals from 10 minutes to 1 hour (see, for example, [5]).

4. – Comparison of ECMWF forecasts with local observations

With the aim of verifying the reliability of ECMWF forecasts at the location of ESO observatories in Chile, we proceeded essentially in the same way as in the comparisons of ECMWF analysis described in the previous section. In such way we evaluated the worsening of forecast fields of interest with respect to the analysis.

4.1. Vertical profile comparisons. – We performed a systematic comparison of vertical radiosoundings of temperature and wind velocity of balloons released daily at 12 GMT in Antofagasta and Quintero in 1993 with the corresponding variables derived from ECMWF 24- and 48-hour forecasts. The results of this comparison, together with

the results previously found with ECMWF analysis and discussed in the previous section, are summarized in table II in terms of average values of correlation, mean error, and mean absolute error for temperature and wind velocity profiles. This kind of comparison was also extended, for temperature profiles, to the shole radiosounding dataset of the 5-year period from 1989 to 1993 (see again table II). It can be observed that the mean error of the analysis is about 2.5 degrees, while for the 24-hour forecast it is about 3 degrees: the worsening in the global score of the forecast is only half a degree with respect to the analysis. This probably means that the greatest part of the errors in temperature forecasts can be attributed to the coarseness of the observational network and not to the ECMWF forecast model, since the analysis is used as an initial condition for the forecast. Again, by comparing wind velocity profiles from radiosoundings with those obtained from ECMWF forecasts we found anomalies similar to those exhibited by the ECMWF analysis, that were already shown in fig. 4.

Since conditions of very strong wind (wind speed at telescope level exceeding 15–20 m/s) can cause the closure of the telescope dome and, consequently, the interruption of astronomical observing activities, we focused our attention on errors in the evaluation of strong winds in ECMWF vertical profiles. In particular, we computed the following average relative error of each daily vertical profile:

$$(1) \quad \varepsilon_w(\text{day}) = \frac{1}{N} \sum_N \left| \frac{V_{\text{ECMWF}} - V_{\text{SOUND}}}{V_{\text{SOUND}}} \right|,$$

where V_{ECMWF} is the velocity derived from ECMWF analysis or forecast, while V_{SOUND} is the radiosounding velocity measured by balloons released in Antofagasta and Quintero.

Relative errors of wind speed were estimated, in the range of interest for this study and for the aim of ESO, by imposing the condition that in each term of the summation (1) the ECMWF velocity (V_{ECMWF}) or the radiosounding velocity (V_{SOUND}) were greater than 10 m/s, and therefore N is the number of terms in each profile in which at least one velocity (or both) satisfy this criterion. Table V reports the scores obtained during 1993 and during the 5-year period 1989–93. The bad results for Quintero 1993 are certainly related to the anomalous period after March 1993. In the case of wind the results are worse than for temperature: the errors for the 24-hour forecast are considerably larger than for the analysis. The main cause is probably to be found in the smoothed description of orography at the spatial resolution of the ECMWF forecast model.

TABLE V. – *Extreme wind events (velocities bigger than 10 m/s): averages of daily relative errors of radiosounding wind velocity against ECMWF analysis and 24/48-hour forecast during 1993 period and during the 1989–93 period.*

	Antofagasta		Quintero	
	1993	89–93	1993	89–93
Analysis	20%	21%	52%	31%
24 h for.	48%	46%	98%	62%
48 h for.	63%	58%	118%	80%

TABLE VI. – *Correlations (r), mean errors ($\bar{\epsilon}$), and mean absolute errors ($|\bar{\epsilon}|$) between 2-meter temperature observations at La Silla and Paranal during the 1989–93 period and values interpolated from 24/48-hour ECMWF forecast of upper-air temperature.*

Station	Model	$\bar{\epsilon}$	$ \bar{\epsilon} $	r
Paranal at 12 GMT	24 h ECMWF forecast	– 0.1	1.3	0.83
	48 h ECMWF forecast	– 0.2	1.4	0.80
La Silla at 12 GMT	24 h ECMWF forecast	– 1.2	1.7	0.90
	48 h ECMWF forecast	– 1.2	1.7	0.88

4.2. Two-meter temperature comparisons. – In table VI we show results of comparison between observed 2-meter temperature and the ECMWF 24-48 hour forecast of temperature. The compared values were computed at the same altitude of the station of interest using the vertical profile bilinearly interpolated from the ECMWF upper-air temperature field. For reasons already discussed in the previous section, results of direct comparisons with ECMWF 2-meter temperature fields are not presented here. It can be seen that the mean absolute error is, in general, greater than that obtained by comparing observations and analysis: in particular, for 24-hour forecasts it is about 1.3 degrees for Paranal and 1.7 degrees for La Silla.

5. – Possible improvements of ECMWF forecasts by means of Kalman filter post-processing

Given the absence of advanced observational meteorological facilities (radar, wind profilers, etc.) at the sites of the ESO observatories, we have tested two standard tools for possible improvement of the local forecast: statistical “post-processing” and the nesting of a LAM into the ECMWF global forecast model. Results of the LAM application to selected test cases will be presented in the next section, while in this section we discuss the improvement obtained using the Kalman filtering procedure described in detail in [3] in relation to the post-processing of a meteorological model output.

Use of Kalman filtering as a post-processing tool is aimed at filling, by means of statistical information, the gap between large-scale dynamics computed by the numerical model and local evolution of the meteorological variables. This is usually done by applying some scheme of statistical regression between long series of observations of the variables of interest at the considered site and some so-called “predictors” (usually the numerically predicted values of the same variables at neighbor points in the numerical grid).

It is well known that the output of a numerical model is affected by systematic errors which can be due, for example, to errors in the physical parameterizations and/or initialization, and to unresolved sub-grid processes and local effects. For this reason, in the last few years operational meteorological centers throughout the world have applied post-processing methods aimed at filtering out noise and systematic errors by using some sort of dynamical self-adaptive regression method (see, for example, [6-9]). One of the best known among these methods is the Kalman filtering procedure.

TABLE VII. – Absolute mean errors ($|\overline{\varepsilon_0}|$) and correlations (r_0) between observed 2-meter temperatures (T2m) or 10-meter wind (W10m) and estimations by Kalman filter post-processing ($\circ = \text{Kal}$), persistence ($\circ = \text{per}$), ECMWF 24-hour forecast ($\circ = \text{for}$), and ECMWF analysis ($\circ = \text{ana}$) at 12 GMT. N is the number of data used for comparison during the period from 1989 to 1993. The small differences with respect to tables IV and VI are due to the different number of values used.

Field	Site	N	$ \overline{\varepsilon_{\text{Kal}}} $	r_{Kal}	$ \overline{\varepsilon_{\text{per}}} $	r_{per}	r_{for}	r_{ana}
T2m (C)	Paranal	572	1.1	0.88	1.5	0.80	0.79	0.87
	La Silla	1114	1.6	0.86	2.1	0.77	0.82	0.86
W10m (m/s)	Paranal	608	3.0	0.59	3.4	0.56	0.50	0.64
	La Silla	1242	2.5	0.64	2.9	0.59	0.57	0.43

We applied the Kalman algorithm to the post-processing of ECMWF fields in order to predict 2-meter temperature at 12 GMT, for Paranal and La Silla. The validation is made by using surface observations in these two sites, during the period from 1989 to 1993, and ECMWF forecast and analysis of upper-air temperature interpolated at the station: vertically (at the altitude) and horizontally (at the position).

Results are shown in table VII. In comparison with the persistence, which gives an indication of the daily variability of the parameter, we obtain an improvement of the absolute mean error of about 0.5 degrees. Correlation coefficients are high and equal to those of the analysis. In the table we do not show the mean absolute errors of analysis and forecast because they are affected by very large systematic errors not comparable with those of the post-processing. In particular, during daytime, 2-meter temperatures, obtained by interpolation of upper-air temperature from ECMWF analysis and forecast, are systematically lower than measured temperatures because of the contribution of the ground radiation to air temperature.

For this reason we have also tried to make the same comparison by using at once ECMWF forecast and analysis of 2-meter temperature as predictors, in place of vertically interpolated values of upper-air temperature fields. The results are much worse than those in table VII. Essentially, this is due to the fact that the parameterization of ground physics and planetary boundary layer of the ECMWF GCM is referred to properties of the ground (as orography, roughness, soil temperature, etc.) that are representative for the grid resolution of the model, and so completely inadequate to correctly describe the local dynamics at the station sites.

To evaluate the improvement due to the KF procedure with respect to zero knowledge (persistence), we summarize the skills of both procedures in table VIII. For conciseness, and because the results for La Silla are very similar, only the results for Paranal are shown. Looking at the last column of the table, we see that the number of times the error of the KF procedure in forecasting 2-meter temperature within an absolute error of 1 degree is $159+158=317$ (55% of the total number of data used in table VIII). At the same time the number of times the error of the persistence is within the same range is $112+117=229$ (40%). The forecast of the external temperature with an error less than 1 degree is a desired condition for astronomers, as it allows to preset the air conditioning in the telescope room, assuring that the mirror is completely operational at the opening of the dome. It is apparent that there is a sensible added

TABLE VIII. – Contingency table between 2-meter temperature errors of the Kalman filtering post-processing procedure (KFPP) and of the “24h persistence model” at Paranal during the period 89–93 at 12 GMT. The sum of the counts along rows (shown in the last column of the table) is the number of times the 2-meter temperature has been forecast by KFPP within an error indicated in the first column of the table itself. The sum of the numbers along a column (shown in the last row) is the number of times the 2-meter temperature has had a diurnal variation within the value shown in the first row. The generic count within a cell of the table gives the number of times the 2-meter temperature has been forecast within an error indicated in the corresponding cell of the first columns when the daily variation of the 2-meter temperature was that indicated in the corresponding cell of the last row.

		Persistence errors (K)													
		-6	-5	-4	-3	-2	-1	1	2	3	4	5	6		
KFPP errors (K)	-6	0	0	0	1	1	0	0	0	0	0	0	0	2	Global scores of KFPP
	-5	0	0	0	0	0	0	0	0	0	0	0	0	0	
	-4	0	1	1	4	2	1	0	0	0	0	0	1	10	
	-3	0	1	3	8	9	3	3	2	1	1	0	0	31	
	-2	1	2	11	14	17	22	9	3	0	0	0	0	79	
	-1	1	5	3	14	38	38	34	15	9	2	0	0	159	
	1	2	2	2	4	15	34	47	28	16	5	3	0	158	
	2	0	0	2	1	5	9	21	15	18	5	5	2	83	
	3	0	0	0	0	4	5	2	6	10	1	2	3	33	
	4	0	0	0	0	0	0	1	3	4	2	1	1	12	
5	0	0	0	0	0	0	0	1	0	1	1	0	3		
6	0	0	0	0	0	0	0	0	1	0	0	1	2		
		4	11	22	46	91	112	117	73	59	17	12	8	Global scores of persistence	

value in using the KF procedure, quantifiable as the increase in the number of operational days $317 - 229 = 88$ (15%).

The same procedure was applied to 10-meter wind speed giving the results shown in table VII, but some clarification is needed about the contents of this table and about comparison of wind components in general. First of all it should be clear that any direct comparison between wind components cannot be proposed because the wind at ground level is heavily influenced by orographic effects (characteristic scale of hundreds of meters) that are several orders of magnitude lower than that in the orography of the

TABLE IX. – Contingency counts between measured 10-meter wind speed and Kalman filter post-processing, for La Silla. The total number of data points is 1242 for the period from 1989 to 1993.

		V (m/s)	Kalman filter estimates				
			0–5	5–10	10–15	15–20	20–25
Measured	0–5	392	137	17	3	0	
	5–10	172	250	99	13	1	
	10–15	4	50	59	21	2	
	15–20	2	2	10	5	2	
	20–25	0	0	0	0	1	

model (~ 10 km). This is reflected especially in wind direction and for this reason we have not considered it. Wind speed may be less influenced by these, in any case strong, orographic effects and so for this variable we performed the same analysis as already performed for 2-meter temperature.

As can be seen in table VII, the mean absolute error of 10-meter wind speed after Kalman filtering is about 3 m/s, which must be compared with the mean value of the field, 7 m/s. Correlations are about 0.6: small, but in any case greater than correlations of forecast and analysis. It is evident, however, that analysis and forecast are very poor because correlations are small and not statistically significant: for example, in La Silla the correlation of forecast is greater than the correlation of analysis.

To evaluate the relevance of these results to the specific aims of the ESO astronomers, we show in tables IX and X contingency between measured and Kalman filtered data for five classes of wind speed from 5 m/s to 25 m/s in Paranal and La Silla. The winds belonging to the two classes from 0 to 10 m/s, which give no problems to the astronomers, are forecast correctly 75% of the time and are present 85% of the time. The two classes between 10 and 20 m/s are forecast correctly 8% of the time and are present 15% of the time. More interesting is the analysis of the class of wind speed greater than 20 m/s, on occurrence of which the telescope cannot be used. It must, first of all, be noted that the number of occurrences of this event is very low: only 1 in La Silla and 6 in Paranal. In any case the corresponding post-processed values are not in

TABLE X. – Contingency counts between measured 10-meter wind speed and Kalman filter post-processing, for Paranal. The total number of data points is 608 for the period from 1989 to 1993.

		V (m/s)	Kalman filter estimates				
			0–5	5–10	10–15	15–20	20–25
Measured	0–5	135	61	10	1	0	
	5–10	103	118	61	14	1	
	10–15	1.5	26	25	18	0	
	15–20	0	1	10	6	3	
	20–25	0	2	1	3	0	

good agreement. From these results it seems that forecasts of ground wind speed from a GCM would not be useful to ESO astronomers.

As already mentioned, ECMWF analysis during the period 1992-93 shows consistently large errors, probably due to the Quintero balloon data. To check the influence of this anomalous period in our analysis of the Kalman filtering procedure, we repeated all the calculations described in this section using only data for the period 1989-1991. The results were very similar to those reported in table VII for the whole period 1989-93. Some differences were observed for correlations of analysis and forecast of temperature: in particular, we have found for La Silla in the shorter period $r_{\text{for}} = 0.87$ and $r_{\text{ana}} = 0.91$ which are greater than the corresponding values in table VII. This could be an indication that the analysis, and therefore the forecast, were better during the shorter period. We remark, in conclusion, that the performances of the Kalman filtering procedure are not influenced by the apparent worsening of the analysis during the period 1992-93.

6. - Discussion of LAM test cases

In this section we discuss results of application of a LAM in a limited region including Chile, giving particular emphasis to forecasts of 2-meter temperature and 10-meter wind at Paranal and La Silla. A general description of the core equations (dynamic equations) and some detail of the numerical aspects of the LAM we used can be found in [10,11], while for the parameterizations of the sub-grid processes (characterized by typical spatial scales smaller than the model resolution, such as vertical diffusion, dry adiabatic adjustment, soil water and energy balance, large-scale precipitation and evaporation, moist convection and radiation) the reader can refer directly to ref. [12-16].

The fields used as initial and boundary conditions needed to solve the equations of motion for atmospheric dynamics are obtained from a GCM, provided by the ECMWF in our case. Generally, one has to deal with an analysis obtained by interpolating observations from various sources (such as ships, aircrafts, balloons, satellites and meteorological stations) and “initializing” such interpolated fields in order to filter out dynamical noise and to make these fields consistent with the GCM equations of motion [17]. The ECMWF initialized analysis and the model forecasts (06 to 120 hours at 6-hour intervals, 120 to 240 hours at 12-hour intervals) are disseminated to regional meteorological centers via a dedicated telecommunication network, at four analysis times (18 GMT preceding day, 00, 06, 12 GMT current day). Since initial and boundary conditions are dynamically consistent with the equation of the GCM, their interpolation to the grid of the LAM (pre-processing) will produce in the first hours of integration spurious non-physical waves which are, however, rapidly damped by applying a numerical diffusion and also by using a proper relaxation procedure between LAM forecasts and time-dependent lateral boundary conditions [18, 19].

Some simulations were performed in order to evaluate the LAM performance on the region of interest. All the numerical integrations were performed using a horizontal grid with resolution of one sixth of degree (latitude step ~ 17 km, longitude step ~ 15 km), on 93 longitude grid points (from 279.75E to 295.08E), 100 latitude grid points (from 18.58S to 35.25S) and 20 vertical levels on sigma coordinates. In fig. 2 the LAM orography, obtained from an NCAR (National Center for Atmospheric Research) digital elevation map, is plotted and compared with that at 0.5625 degree resolution of

ECMWF model, while in fig. 3 the corresponding W-E sections of orography at Paranal latitude are shown. The time step used for the integration of the dynamic equations was 15 seconds, while a 10-minute time step has been used for the contributions of physical parameterizations like radiative transfer, large-scale precipitation, and vertical convection.

Initial and boundary conditions needed for LAM simulations were obtained from interpolation of the ECMWF analysis at one sixth degree resolution on each of the 20 sigma levels. After integrations, we used a standard “post-processing” procedure to interpolate the model variables from sigma levels to standard isobaric levels and to account for surface processes [20]. In the “post-processing” phase some new “surface” fields, such as the 2-meter air temperature and 10-meter wind, were also computed.

We produced 5 different test cases, each one with time of forecast of 72 hours, in order to estimate LAM capability to predict local observations at the Paranal and La Silla meteorological stations:

– 3 test cases, starting at 00 GMT on 04/03/93, 12/05/93 and 20/05/93, were selected during cyclogenetic perturbations. In particular, during the 2 test cases of May, the southern hemisphere jet stream was very close to the southern boundary of the domain used for the integration. In fig. 5a, b, c the 500 mb geopotential heights after 1 hour, 24, 48, and 72 hours of integration for each simulation are plotted.

The case starting on 04/03/93 is a case of weak penetration of a middle-latitude trough (the core of the trough appears in the LAM domain only in the last day of integration). Analysis shows interaction of the westerly jet stream with the Andes, with an initial tendency to flow splitting (particularly pronounced on March 4) and strong generation of orographic waves on successive days in which the reinforced jet stream flows across the Andes; as already mentioned, only in the last day does the extratropical cyclone enter the LAM domain.

– 1 test case, starting at 00 GMT on 17/08/93, was selected as in that period a great difference between the temperature observed in Paranal and that of ECMWF analysis and forecast was found. In fig. 5d the 500 mb geopotential height maps for this test case are plotted.

– 1 test case, starting at 00 GMT on 18/03/93, was selected as representative for periods in which nothing of meteorological interest happens, as can be seen from fig. 5e where the 500 mb geopotential height maps are plotted.

We have compared 2-meter air temperature and 10-meter wind velocity measured at meteo-stations in Paranal and La Silla with numerical values from the LAM forecasts in the above 5 test cases. In these comparisons we have used both “surface” values and “upper air” values (horizontally interpolated at the station location, and vertically at station altitude) of 2-meter temperatures and 10-meter winds.

LAM integrations were saved every hour (total of 72 hours for each test case), but we compared only values during the Chilean night from 00 GMT to 10 GMT (that is the time interval of interest for astronomical activity). In fig. 6 and 7 values of 2-meter temperature and 10-meter wind speed observed in Paranal and La Silla are plotted vs. “surface” or “upper air” values obtained by LAM forecast. In tables XI and XII errors of 2-meter temperature in Paranal and La Silla from ECMWF analysis and from the LAM “upper air” forecast are compared. It must be pointed out that great errors in ECMWF fields are often reflected also in the LAM forecast.

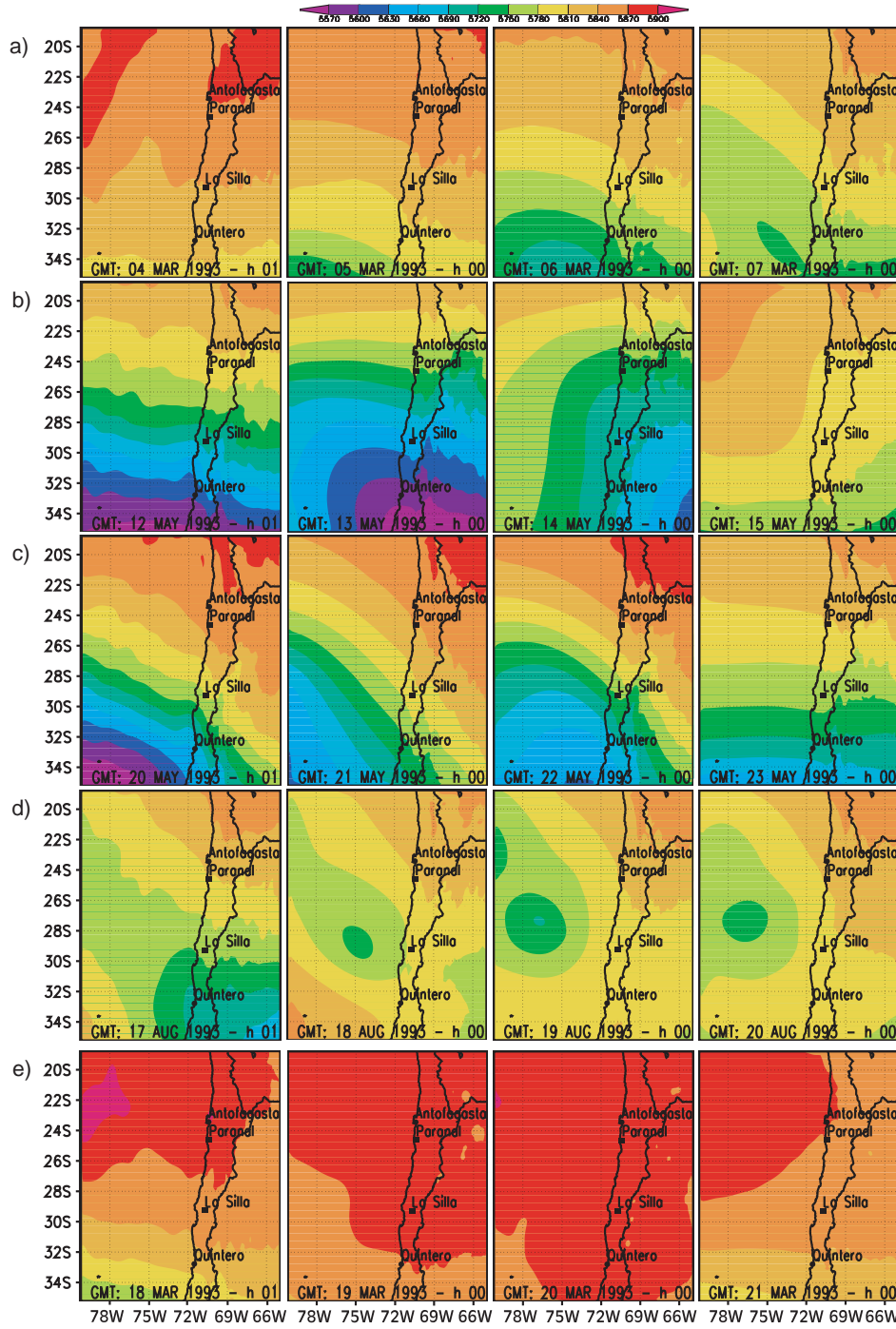


Fig. 5. - Forecast of geopotential height (meters) at 500 mb after 1 hour, 24, 48, and 72 hours by LAM integration with a one sixth degree orography (see fig. 2, right) started at 00 GMT on: a) 4 March 1993, b) 12 May 1993, c) 20 May 1993, d) 17 August 1993, e) 18 March 1993.

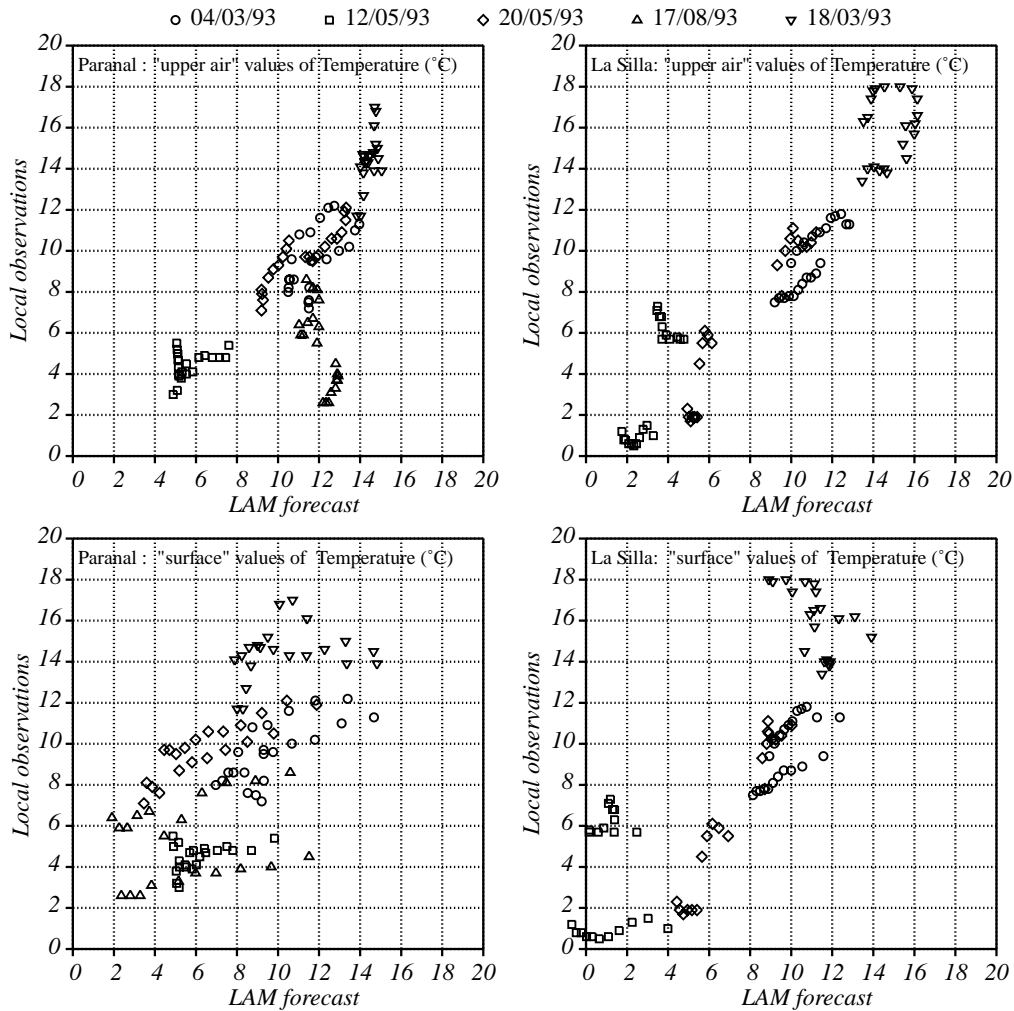


Fig. 6. – Scatter-plots of 2-meter air temperature observed at Paranal and La Silla vs. estimates based on LAM “upper air” or “surface” values for the five test cases.

We do not analyze in further detail the test case starting on 17/08/93, since we found on 18/08/93 a difference of about 8 degrees between the 2-meter temperature observed in Paranal and the values estimated by ECMWF analysis. For the remaining cases the LAM predictions of temperature seem to be in general quite good, in particular if the “upper air” values are used. Also the wind velocity forecast is better when using “upper air” values rather than “surface” values. This suggests that, for operational use of a high-resolution meteorological numerical model, improvement and specialization of post-processing techniques are certainly needed.

In particular, in the case starting on 04/03/93, the LAM forecast tends to underestimate the initial jet-splitting and to overestimate orographic wave production; both features may be due to inadequate observational coverage and initialization, rather than to inadequacy of the LAM itself. The final penetration of the trough-core is

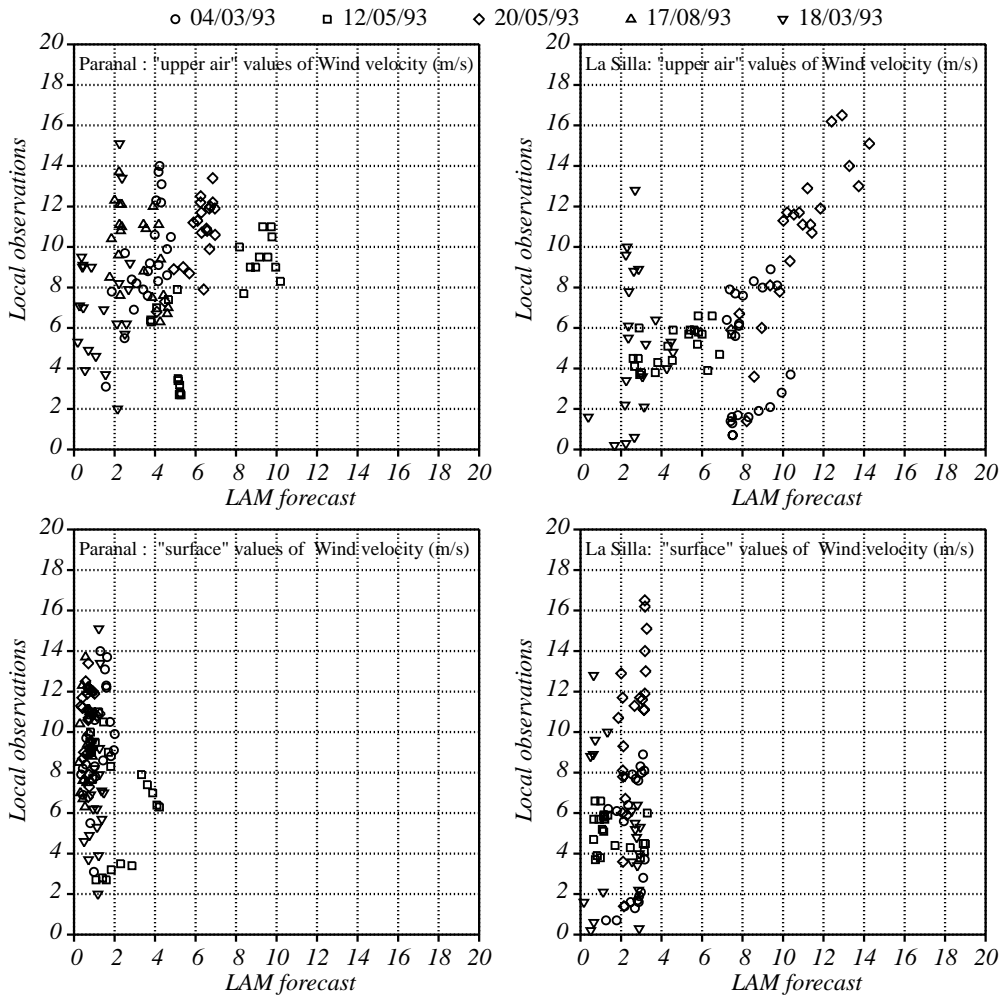


Fig. 7. – Scatter-plots of 10-meter wind velocity observed at Paranal and La Silla vs. estimates based on LAM “upper air” or “surface” values for the five test cases.

well simulated, but this success is probably due to the fact that the cyclonic feature is “forced” through the southerly boundary by the boundary conditions.

Some features are in common to all the numerical experiments performed with the LAM; the most relevant are:

- the horizontal extent of the LAM domain is too small in comparison with the size of extratropical cyclones occasionally deepening equatorward up to the point of hitting the geographic area in question;
- observations are so sparse (in particular, over the Pacific Ocean) that it is presently impossible both to fully exploit and to adequately check the LAM performance;

TABLE XI. – *The 2-meter temperature at Paranal: LAM forecast errors ($\varepsilon_{\text{lam}} = T_{\text{lam}} - T_{\text{observed}}$) and ECMWF analysis errors ($\varepsilon_{\text{ana}} = T_{\text{analysis}} - T_{\text{observed}}$) for the 5 test cases discussed in the text.*

		Forecasting time			
		24	30	48	54
04/03/93	ε_{lam}	2.66	2.10	0.55	1.07
	ε_{ana}	2.43	2.54	-0.34	0.75
12/05/93	ε_{lam}	2.20	1.74	0.12	0.85
	ε_{ana}	2.34	2.28	0.23	2.07
20/05/93	ε_{lam}	1.34	2.09	0.03	****
	ε_{ana}	0.58	1.93	-1.47	****
17/08/93	ε_{lam}	2.78	5.00	8.31	****
	ε_{ana}	3.05	5.93	8.47	****
18/03/93	ε_{lam}	0.39	-0.44	1.15	-0.56
	ε_{ana}	0.36	0.13	0.32	-0.67

– strong trains of gravity-inertia waves appear in all the LAM forecasts in the lee side of the Andes. These are probably in part real (the improved resolution allows description of the gravity-inertia dynamics which is smoothed in the ECMWF analysis and forecast) and in part due to the effect of sub-grid (with respect to ECMWF grid size) orography in the initialization procedure.

TABLE XII. – *The 2-meter temperature at La Silla: LAM forecast errors ($\varepsilon_{\text{lam}} = T_{\text{lam}} - T_{\text{observed}}$) and ECMWF analysis errors ($\varepsilon_{\text{ana}} = T_{\text{analysis}} - T_{\text{observed}}$) for the 5 test cases discussed in the text.*

		Forecasting time			
		24	30	48	54
04/03/93	ε_{lam}	1.53	0.49	2.03	2.33
	ε_{ana}	0.36	0.55	0.74	1.30
12/05/93	ε_{lam}	2.28	1.61	-2.00	-2.59
	ε_{ana}	0.49	-0.31	-1.91	-0.16
20/05/93	ε_{lam}	0.32	-1.01	0.63	3.39
	ε_{ana}	-0.82	-2.73	-0.08	1.73
18/03/93	ε_{lam}	-0.16	-3.80	0.24	0.52
	ε_{ana}	-1.30	-2.75	-0.73	-0.09

7. – Summary and concluding remarks

We summarize here the more relevant results of our comparative study of some ECMWF fields, such as cloud cover, temperature, and wind, against the corresponding observations at the sites of European astronomical facilities in Chile.

Different criteria of estimation of cloud cover in Paranal from ECMWF analysis have revealed only a marginal improvement with respect to the simple assumption, justified by the geographical location of Paranal, that the sky is always clear. Due to the poor results obtained with the ECMWF analysis, the comparisons were not extended to the 24/48-hour forecast fields of the ECMWF dataset.

By comparing vertical profiles of temperature from radiosoundings at Antofagasta and Quintero with profiles obtained from the ECMWF analysis we found a mean absolute error of about 2.5 degrees. The corresponding comparison performed with vertical profiles from 24-hour ECMWF forecasts revealed a mean absolute error of about 3 degrees. This difference of only half a degree with the error of the analysis means that a large part of the temperature errors in the vertical profiles extracted from the ECMWF 24-hour forecast is probably due to inadequate knowledge of the “initial condition”, namely the analysis, for the ECMWF general circulation model.

Comparisons between vertical profiles of wind velocities from radiosoundings with the corresponding ECMWF fields were, instead, very poor, in terms of both correlations and absolute errors. Further investigations, focused on extreme wind conditions (wind velocities higher than 10 m/s), revealed a mean absolute error of about 50% in the 24-hour ECMWF forecast profiles against an error of 25% for the corresponding analysis profiles.

Two-meter temperatures measured at the meteorological stations at Paranal and La Silla were compared with the corresponding estimates based on the 2-meter temperature fields and upper-air 3D temperature fields from the ECMWF analysis. The comparison with the 2-meter temperature of ECMWF analysis have revealed very large errors, even larger than errors of the persistence model. The cause of these discrepancies can be essentially attributed to the smoothed representation of the orography in the ECMWF grid: the geopotential height of the ECMWF model at the location corresponding to Paranal and La Silla is very different from the real one.

Better results were instead found by interpolating the ECMWF 3D temperature field at the same geographical location and altitude of the meteorological sites obtaining a mean absolute error of about 1.3 degrees at Paranal and 1.7 degrees at La Silla. Since a systematic error was still present, a statistical post-processing tool, based on the Kalman filter algorithm, was applied to the 24-hour forecast. The Kalman filter was designed to take into account not only the 24-hour forecast, but also the information coming from actual analysis and local observation. It was able to further reduce the errors in predicting 2-meter temperature to about 1.1 degree at Paranal and 1.6 degree at La Silla. This procedure is currently applied by ESO to temperature, wind speed, and pressure at ground level both in Paranal and La Silla (<http://www.eso.org/genfac/pubs/astclim/forecast/meteo/verification/>).

Finally, some test cases of LAM simulations in Chile were discussed with the aim of evaluating the gain, in terms of 2-meter temperature errors and 10-meter wind velocity errors, when increasing the spatial resolution from the ECMWF grid to a finer grid. Results of this investigation show that also for LAM forecasts the greatest part of larger errors are probably due to inadequacy of the initial conditions obtained

from ECMWF analysis. As we have already found for the other kind of comparisons, the LAM forecast of temperature is better represented than the wind field.

Since the orography of the LAM is completely different from the real one and the LAM grid square is at least 10 km², further statistical post-processing procedures should be applied in order to eliminate systematic geometrical errors. We did not apply the Kalman filter post-processing to the LAM forecasts due to the small amount of data produced with the simulations, but it is clear that it could be successfully applied also to the output of an operative LAM.

Before closing, we want to remark, once again, that analysis and forecasts of all numerical variables considered here suffer from the problem of “downscaling”; in fact, the marginal statistical difference between analysis and forecast is, in itself, an indication that the problems in question already arise in the initialization phase of the forecasting procedure; in this phase the meteorological fields must be interpolated locally starting from observations collected from a very coarse network.

Such downscaling problems can be addressed with different approaches, not necessarily mutually exclusive:

- static (mass-conserving adjustment) and statistical (Kalman filter) post-processing techniques can prove useful in correcting part of the systematic errors, but cannot improve the local forecast in cases of dramatic changes of meteorological fields which are, however, of great importance in the management of astronomical facilities;

- limited area models have the potential for improving the local forecast, but they have to be fed with adequate initial data and extended in space to the middle-latitude westerlies in order to capture the dynamics of troughs that only on occasion penetrate the tropical circulation, but, on these same occasions, cause severe changes in the local weather at the sites of interest.

* * *

This research has been financed by ESO (contract number 45060/VLT/95/6962/GWI) and by the Sardinian Regional Authorities. The authors are very grateful to Prof. ROBERTO BENZI for early guidance in the project, to MARC SARAZIN for interesting and helpful discussions, and to CLAUDIO PANICONI for reviewing the manuscript.

REFERENCES

- [1] SARAZIN M., *Predicting observing conditions at ESO observatories - reality and perspectives*, Technical Report 89, ESO (1997).
- [2] BENZI R., DEIDDA R., MARROCU R. and SPERANZA A., *Feasibility study of a meteorological prediction model for ESO observatories in Chile (phase A1, A2)*, Technical report CRS4-TECH-REP-96/51, CRS4, Cagliari, Italy (1996).
- [3] DEIDDA R., MARROCU R. and SPERANZA A., *Feasibility study of a meteorological prediction model for ESO observatories in Chile (phase A3, A4)*, Technical report CRS4-TECH-REP-97/38, CRS4, Cagliari, Italy (1997).
- [4] DEIDDA R., MARROCU R. and SPERANZA A., *Proposal for a system of operational forecast finalized to meteorological prediction for ESO observatories in Chile (phase A5)*, Technical report CRS4-TECH-REP-97/56, CRS4, Cagliari, Italy (1997).

- [5] RATTO C. F., FESTA R., ROMEO C., FRUMENTO O. A. and GALLUZZI M., *Environ. Software*, **9** (1994) 247.
- [6] SIMONSEN C., *Self adaptive model output statistics based on Kalman filtering*, Technical report, Danish Meteorological Institute (1991).
- [7] CACCIAMANI C. and DE SIMONE C., *Minimum temperature forecasts at the regional meteorological service of the Emilia Romagna region (North Italy) by the application of the Kalman filter technique*, *ECMWF Newslett.*, **60** (1992) 9.
- [8] PERSSON A., *Kalman filtering. A new approach to adaptive statistical interpretation of numerical meteorological forecasts*, *ECMWF Newslett.*, **46** (1989) 16.
- [9] CATTANI D., *Application d'un filtre de Kalman pour adapter les temperatures a 2 metres fournies par le modèle ECMWF aux station météorologiques de la Suisse*, Technical report No. 175, ISM (1994).
- [10] BUZZI A., FANTINI M., MALGUZZI P. and NEROZZI F., *Meteorol. Atmos. Phys.*, **53** (1994) 137.
- [11] MARROCU M., SCARDOVELLI R. and MALGUZZI P., *Parallel Comput.*, **24** (1998) 911.
- [12] CHARNOCK H., *Q. J. R. Meteor. Soc.*, **81** (1955) 639.
- [13] EMANUEL K. A., *J. Atmos. Sci.*, **48** (1991) 2313.
- [14] GELEYN J.-F. and HOLLINGSWORTH A., *Contrib. Atmos. Phys.*, **52** (1979) 1.
- [15] LOUIS J.-F., TIEDTKE M. and GELEYN J.-F., *A short history of the PBL parameterization at ECMWF*, in *Proceedings from the ECMWF Workshop on Planetary Boundary Layer Parameterization, 25-27 November 1981* (ECMWF, Reading, UK) 1982, pp. 59-79.
- [16] RITTER B. and GELEYN J.-F., *Mon. Weath. Rev.*, **120** (1992) 303.
- [17] DALEY R., *Rev. Geoph. Space Phys.*, **19** (1981) 450.
- [18] DAVIES H. C., *Q. J. R. Meteor. Soc.*, **102** (1976) 405.
- [19] KÄLLBERG P., *Test of lateral boundary relaxation scheme in a barotropic model*, Technical report No. 3, ECMWF (1977).
- [20] GELEYN J.-F., *Tellus A*, **40** (1988) 347.